Pergamon

Int. J. Heat Mass Transfer. Vol. 39, No. 8, pp. 1555–1567, 1996

0017–9310/96 $15.00 + 0.00

0017–9310(95)00273–1

Creeping flow of a Bingham plastic through axisymmetric sudden contractions with viscous dissipation

KHALED J. HAMMAD and GEORGE C. VRADIS†

Department of Mechanical Engineering, Fluid Mechanics Laboratory, Polytechnic University, Brooklyn, NY 11201, U.S.A.

(*Received* 6 *April* 1995 *and in final form* 14 *July* 1995)

Abstract—The effects of the yield number on the steady, incompressible creeping flow of a non-Newtonian Bingham fluid through a four-to-one axisymmetric sudden contraction is studied numerically. The effects of both the yield and Peclet numbers on the thermal field, created due to the viscous dissipation associated with such flows, are investigated. The results demonstrate the dependency of the flow field on the yield number and the strong influence of both the yield and Peclet numbers on the macroscopic and local characteristics of the thermal field. The heat transfer results indicate the significance of heating via viscous dissipation, especially in the vicinity of the contraction plane at high yield numbers.

INTRODUCTION

The flow through axisymmetric sudden contractions has attracted considerable attention because it is encountered in numerous industrial applications, including the extrusion of polymeric fluids and melts. This same flow has also been used frequently as a benchmark problem in computational fluid mechanics and heat transfer. Its geometrical simplicity and hydrodynamic complexity make it an ideal problem for testing various numerical methods as well as validating the constitutive equations used to characterize the rheology of non-Newtonian fluids. As a result a wealth of literature exists on such a flow covering a wide range of fluids and governing parameters.

Figure 1 shows the basic characteristics of the flowfield under consideration. Assuming a long enough pipe element upstream, the flow at a small distance upstream of the contraction can be assumed to be fully developed. In the case of a Newtonian fluid, as the contraction plane is approached, the flow field is disturbed resulting in the formation of a recirculating flow region at the 90 degree corner. The extent of this region is strongly dependent upon the two governing parameters, i.e. the Reynolds number Re which is the flow parameter and expansion ratio β which is the geometrical parameter. At the throat the flow accelerates as it enters the smaller pipe, where another separated flow region could form depending again on both the flow and geometric parameters. Therefore, the flow continues developing until fully developed conditions are eventually reached further downstream.

In the case of Newtonian fluids, numerous previous studies have concentrated on the effect of both the contraction ratio and the Reynolds number on the flow structure. These studies include the experimental works of Burke and Berman [1] and Ramamurthy and McAdam [2]. A limited review of both experimental and computational work is given by Boger [3]. The size of the corner recirculating flow region increases with increasing contraction ratio and decreasing Reynolds numbers. However, once the Re is in the creeping flow range and β is greater than four the size of this region remains unchanged. For higher Reynolds numbers the streamwise velocity profile at the entrance of the downstream pipe shows concavities, absent in creeping flows. Numerous experimental and computational studies have established the features of such a flow to the point where Boger [3] considers it 'solved'.

Numerous studies have concentrated on the structure of such a flow for various non-Newtonian fluids. Kim-E *et al.* [4] presented results for an inelastic shear-thinning Carreau fluid. Their results indicate that increasing shear thinning reduced the size of the recirculating flow region and increased the entrance pressure losses. A number of review papers like those of Boger [3] and White *et al.* [5] discuss the characteristics of the flowfield in the case of elastic fluids. Increasing Deborah numbers (De), i.e. increasing elastic effects, result in the enlargement of the corner vortex and eventually in the onset of three-dimensional (3D), highly localized, temporal instabilities.

Fluids exhibiting a yield stress are frequently encountered in numerous applications related to the plastics, food, petroleum and pharmaceutical indus-

† Author to whom correspondence should be addressed. Present address: Mechanical Engineering Department, Polytechnic University, Route 110, Farmingdale, NY 11735, U.S.A.

NOMENCLATURE

C_f	friction coefficient, $\tau_w/\rho U_i^2$
D	diameter of the upstream pipe
d	diameter of the downstream pipe
k	thermal conductivity
L_d	detachment length
L_e	entry length
Nu	Nusselt number based on bulk temperature, $[(\partial\theta/\partial r\|_{r=1})/\theta_b]$
Pr	Prandtl number, $\eta/\rho a$
Pe	Peclet number, $Re\ Pr$
p	non-dimensional pressure, $P/\rho U_i^2$
P	pressure
r	non-dimensional radial distance, R/R_w
r_0	non-dimensional 'core' radius, R_0/R_w
R	radial distance
R_0	radius of the 'core'
R_w	radius of the upstream pipe
Re	Reynolds number, $\rho d U_i/\eta$
T	temperature
u	non-dimensional streamwise velocity, U/U_i
U	streamwise velocity
v	non-dimensional radial velocity, V/U_i
V	radial velocity
x	non-dimensional streamwise distance, X/R_w
X	streamwise distance
Y	yield number, $\tau_0 R_w/\eta U_i$.

Greek symbols

α	thermal diffusivity
β	contraction radio, D/d
Δ_{ij}	rate of deformation tensor, $(\partial u_i/\partial x_j)+(\partial u_j/\partial x_i)$
η	plastic viscosity
θ	non-dimensional temperature, $(T-T_i)/(\eta U_i^2/k)$
θ_b	non-dimensional bulk temperature, $\int_0^1 u(r)\theta(r)r\,dr$
Φ	viscous dissipation term, $(\mu_{eff}/Pe)\{\frac{1}{2}(\Delta:\Delta)\}$
μ	effective viscosity
μ_{eff}	non-dimensional effective viscosity, μ/η
ρ	density
τ_{ij}	stress tensor element
τ_0	yield stress.

Subscripts

c	centerline
i	inlet, indicating bulk properties
w	wall.

tries. From all such fluids the simplest rheology is that of a Bingham fluid which exhibits a linear stress-rate-of-strain relationship once the yield stress has been exceeded. Yield-power-law fluids (also known as Herschel–Bulkley fluids) are another class of yield stress exhibiting fluids. Their study is of considerable importance both from a rheological and fluid mechanics point of view. It is only recently however, that studies have addressed flow fields of Bingham and Herschel–Bulkley fluids of some complexity. The review paper by Bird and Dai [6] summarized the early work in this field. Some experimental and computational studies have followed. Park *et al.* [7] and Wildman *et al.* [8] have reported LDV based experimental results concerning the flow of Herschel–Bulkley slurries through a straight pipe and a gradual concentric contraction respectively. Vradis and Otugen [9] and Scott and Mirza [10] have presented

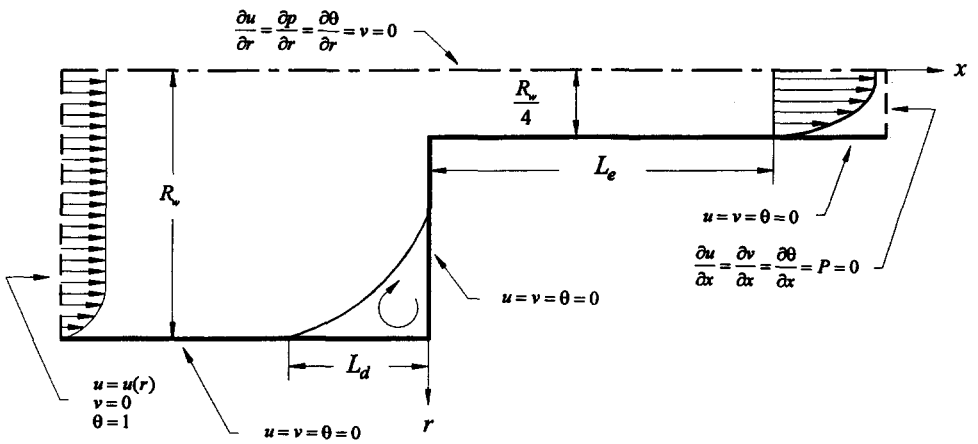

Fig. 1. Geometry and boundary conditions.

numerical solutions to the problem of the flow of a Bingham plastic over a sudden axisymmetric expansion. Isothermal and creeping entry and exit flows through axisymmetric and planar extrusion dies were studied numerically for a Bingham plastic by Abdali and Mitsoulis [11]. In their work, the approximation by Papanastasiou [12] was employed to determine the shape and extent of yielded/unyielded regions, extrudate swell and excess pressure losses as a function of a dimensionless yield stress. No information on the structure of the flow field is given.

In many creeping flows of yield stress fluids a significant portion of the energy needed to maintain the flow is dissipated, mostly in the regions of large shear stresses and large rates of deformation. An understanding of the interaction between the mechanisms of heat transfer, thermal energy storage and dissipation of the flow energy in addition to their ultimate influence on the developing thermal field is of significant practical interest. Viscous heating effects, if large enough, could result in significant increases in temperature which in turn could alter the plastic viscosity, the yield stress and the thermophysical properties of the fluid. This, in return, would reflect on the obtained rheological measurements in the case of rheometry studies and, in the case of extrusion problems, affect the manufacturing process and ultimately product quality. Therefore, the influence of the viscous heating effects on the generated thermal field should be quantified and used to further enhance the reliability of rheological measurements, and to optimize manufacturing processes.

Despite their practical importance non-isothermal studies of flows of Bingham plastics are scarce and limited to flows through simple geometries. The entrance pipe flow and heat transfer problem for a simultaneously developing hydrodynamic and thermal fields have been studied numerically by Samant and Marner [13]. In this numerical study, however, viscous heating and axial conduction were neglected. Vradis *et al.* [14] conducted a comprehensive numerical parametric study of the same problem considering axial conduction and internal heating due to viscous dissipation. In both studies the Nusselt number, Nu, was reported to increase with the yield stress in the fully developed region of the tube. It was also shown that viscous dissipation gives rise to Nusselt numbers that are order of magnitude higher than those obtained when viscous dissipation is neglected. Payvar [15] derived expressions for fully developed temperature profiles and Nusselt numbers for heat transfer in the dissipative flow of a Bingham plastic between parallel plates and through circular pipes. The Graetz–Nusselt problem was extended to a Bingham plastic by Wissler and Schechter [16]. Forrest and Wilkinson [17] presented a theoretical treatment of the heat transfer problem in laminar flows of a Bingham plastic with temperature-dependent properties in circular tubes. In his theoretical analysis, Johnston [18] concluded that in the Graetz problem for a Bingham plastic in laminar tube flow, axial conduction can be ignored for $Pe > 1000$. Non-isothermal recirculating flows as well as flows of a Bingham plastic through a sinusoidal channel were studied by Murty [19]. The problem consisted of a Bingham plastic enclosed in the annular region between a stationary, closed cylinder and an inner rod moving with a constant velocity. In his study Murty utilized a Galerkin's finite element scheme and demonstrated the importance of viscous dissipation in such flows. Assuming a prescribed heat transfer coefficient at the boundaries, Mitsoulis *et al.* [20] carried out inelastic, non-isothermal simulations of the flow of a Herschel–Bulkley fluid through a sudden contraction and presented results showing the extent and shape of yielded-unyielded regions and the development of the temperature field. Furthermore, they used a heuristic approach to determine the level of elasticity required to reproduce the experimental results and showed the appreciable temperature rise due to viscous dissipation.

The present work concentrates on the creeping flow of a viscoplastic, Bingham fluid through a sudden contraction in a pipe under steady, incompressible and laminar flow conditions. There are no reported numerical solutions of the fully elliptic governing equations regarding the detailed flowfield structure of creeping confined flows of Bingham fluids through such a geometry and the thermal field generated due to viscous dissipation. A finite-differences based technique is used for the solution of the elliptic governing equations for mass conservation, momentum balance, and energy conservation. In this study attention is given only to the constant wall temperature case that is set equal to the fluid temperature at the inlet. It is further assumed that the variations of the yield stress, the plastic viscosity, and the thermophysical properties with both temperature and pressure are negligible. This last assumption simplifies the analysis by decoupling the equations of energy and momentum and is justified by the fact that the main intent here is to determine under which conditions the viscous heating is likely to play a significant role. The effect of the yield number on the local and global kinematic properties of the resulting flow field is investigated. The effect of the Peclet number on the characteristics of the thermal field resulting from viscous dissipation is also studied. The contraction ratio is maintained constant throughout this study and is equal to four.

THE GOVERNING EQUATIONS

The non-dimensionalized governing elliptic equations for the non-isothermal, steady, laminar and incompressible flow of a non-Newtonian fluid with temperature independent properties in cylindrical coordinates (written in non-dimensional form) are:

$$\frac{\partial u}{\partial x} + \frac{1}{r}\frac{\partial rv}{\partial r} = 0 \tag{1}$$

$$u\frac{\partial u}{\partial x}+v\frac{\partial u}{\partial r}=-\frac{\partial p}{\partial x}+\frac{1}{Re}\left\{\frac{\partial}{\partial x}\left(2\mu_{\text{eff}}\frac{\partial u}{\partial x}\right)+\frac{1}{r}\frac{\partial}{\partial r}\left(\mu_{\text{eff}}r\left(\frac{\partial u}{\partial r}+\frac{\partial v}{\partial x}\right)\right)\right\} \quad (2)$$

$$u\frac{\partial v}{\partial x}+v\frac{\partial v}{\partial r}=-\frac{\partial p}{\partial r}+\frac{1}{Re}\left\{\frac{1}{r}\frac{\partial}{\partial r}\left(\mu_{\text{eff}}r\frac{\partial v}{\partial r}\right)+\frac{\partial}{\partial x}\left(\mu_{\text{eff}}\left(\frac{\partial u}{\partial r}+\frac{\partial v}{\partial x}\right)\right)-2\mu_{\text{eff}}\frac{v}{r^2}\right\} \quad (3)$$

$$u\frac{\partial \theta}{\partial x}+v\frac{\partial \theta}{\partial r}=\frac{1}{Pe}\left\{\frac{1}{r}\frac{\partial}{\partial r}\left(r\frac{\partial \theta}{\partial r}\right)+\frac{\partial}{\partial x}\left(\frac{\partial \theta}{\partial x}\right)\right\}+\frac{\mu_{\text{eff}}}{Pe}\left\{\frac{1}{2}(\Delta:\Delta)\right\}. \quad (4)$$

The concept of the 'effective viscosity' has been utilized above in writing the governing equations. For a Bingham fluid the effective viscosity μ_{eff} is given by the following formula (Bird *et al.* [21]):

$$\mu_{\text{eff}}=\left\{1+\frac{Y}{\sqrt{(\frac{1}{2}(\Delta:\Delta))}}\right\} \quad \text{for} \quad \tfrac{1}{2}(\tau:\tau)>\tau_0^2 \quad (5a)$$

and

$$\mu_{\text{eff}}=\infty \quad \text{for} \quad \tfrac{1}{2}(\tau:\tau)\leqslant\tau_0^2 \quad (5b)$$

where $Y=\tau_0 R_w/\eta U_i$ is the yield number for Bingham fluids and serves as a non-dimensional yield stress. Here

$$\Delta:\Delta=\sum_i\sum_j \Delta_{ij}\Delta_{ji}$$

is the second invariant of Δ_{ij}. In cylindrical coordinates the functions $\frac{1}{2}(\Delta:\Delta)$ is given by:

$$\tfrac{1}{2}(\Delta:\Delta)=2\left\{\left(\frac{\partial v}{\partial r}\right)^2+\left(\frac{v}{r}\right)^2+\left(\frac{\partial u}{\partial x}\right)^2\right\}+\left\{\frac{\partial v}{\partial x}+\frac{\partial u}{\partial r}\right\}^2. \quad (6)$$

RESULTS

The computational method employed in this study has been used extensively in the past and its accuracy and efficiency is well documented, and is presented in detail by Vradis and Van Nostrand [22]. For this reason it will not be discussed here. However, the computational difficulties associated with the numerical implementation of equation (5b) are discussed next.

In the core regions of the flow the effective viscosity μ_{eff} attains an infinite value since $\Delta=0$. Very large values of μ_{eff} create convergence problems because the coefficient matrix becomes very 'stiff' due to large differences in the magnitude of its elements. In order to avoid such problems, when the value of $\Delta:\Delta$ drops below a certain present level, the effective viscosity μ_{eff} is 'frozen' at a certain relatively high value μ_0, thus warranting convergence. The same approach has been successfully adopted by other researchers in the past (see O'Donovan and Tanner [23] and Lipscomb and Denn [24]). Thus the Bingham plastic rheological behavior is approximated by the following equations:

$$\mu_{\text{eff}}=\left\{1+\frac{Y\left(1-\frac{\eta}{\mu_0}\right)}{\sqrt{(\frac{1}{2}(\Delta:\Delta))}}\right\} \quad \text{for} \quad \tfrac{1}{2}(\tau:\tau)>\tau_0^2 \quad (7a)$$

and

$$\mu_{\text{eff}}=\frac{\mu_0}{\eta} \quad \text{for} \quad \tfrac{1}{2}(\tau:\tau)\leqslant\tau_0^2. \quad (7b)$$

The result of such an approximation is that the rheological behavior of the fluid is altered from that of a Bingham fluid to one with two different viscosities, i.e. a high viscosity of μ_0 at low rates of deformation and a lower value of η at higher rates of deformation. To accurately simulate a Bingham plastic behavior very high μ_0 values should be utilized. The accuracy and computational efficiency of this numerical scheme were found to be quite insensitive to the cutoff value, once this value is greater than $\mu_0=1000\,\eta Y$. In previous work by O'Donovan and Tanner [23] and Beverly and Tanner [25] a 1000 η value for μ_0 was adopted after extensive numerical experimentation. Because of the sharp variations in the values of effective viscosity, strong under-relaxation on the effective viscosity from one iteration level to the next is necessary to obtain convergence.

After extensive studies to establish grid independent solutions, a 39×84 computational grid was employed in the upstream pipe and a 61×21 one in the downstream pipe. The computational domain extended up to $x=-10$ and $x=15$ upstream and downstream of the contraction plane, respectively. The grids were nonuniformly spaced in the streamwise direction, clustered at the inlet section and both upstream and downstream of the contraction plane. The grids in the radial direction were uniformly spaced. This distribution was dictated by the desire to capture the details of both the hydrodynamic as well as the thermal field. The computational domain upstream of the contraction plane was chosen so that a fully developed velocity profile can be used as the inlet condition, while the downstream domain is long enough for both a hydrodynamically and thermally fully developed flow to develop at the exit.

Figure 2 shows the effective viscosity contours for two yield numbers, $Y=10$ and $Y=640$. As shown, the plug regions upstream of the contraction plane are characterized by a high viscosity value. This zone extends further towards the wall as the yield number increases. Another high viscosity zone also appears at the corner in both cases. These high viscosity zones

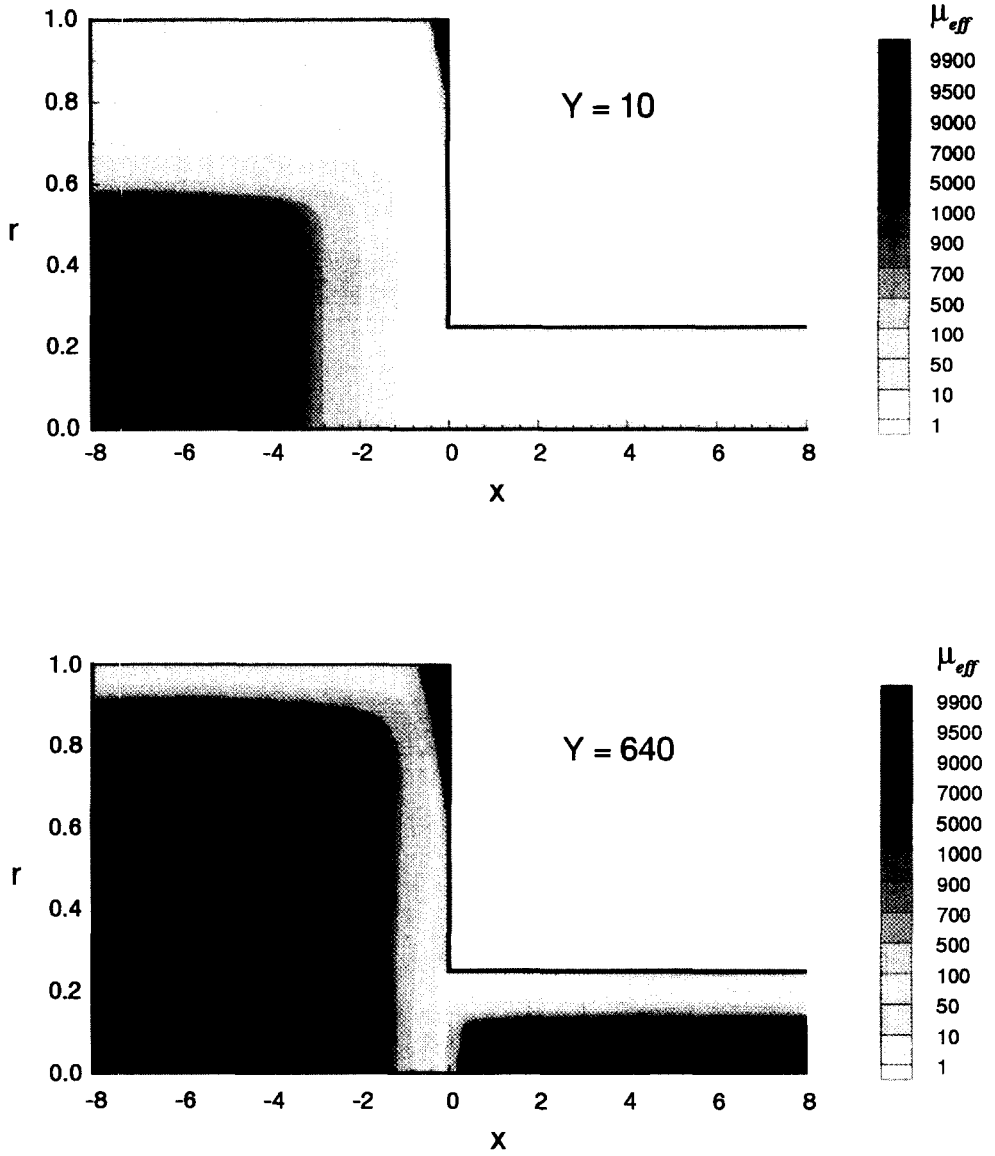

Fig. 2. Contours of effective viscosity for $Y = 10$ and 640.

indicate the existence of a zone of very low rates of deformation. Numerical experimentation indicated that these rates of deformation decrease rapidly with increasing μ_0 and become almost zero for $\mu_0 = 1\,000\,000\ \eta Y$. This strongly suggests a stagnant solid like behavior close to the corner for the limiting case of $\mu_0 = \infty$, i.e. at a real Bingham plastic. For small yield numbers, i.e. $Y = 10$, no plug region is formed in the small diameter pipe. Increasing the yield number to large enough values results in the appearance of another sizeable plug region downstream of the contraction, as shown in Fig. 2(b). The "effective yield number" downstream of the contraction is 1/64 of that upstream of the contraction. Therefore, for small yield numbers the flow in the small pipe is practically Newtonian. Only at higher yield numbers the yield effects become important downstream of the contraction resulting in the formation of the plug region along the centerline. On the other hand, the flow field in the neighborhood of the contraction plane always undergoes large deformation rates which results in a low viscosity zone, regardless of the yield number value. Figure 2 sheds light on the flow field kinematics of a Bingham plastic, indicating a solid like behavior in plug and corner regions, and a similar to Newtonian behavior in the vicinity of the contraction area.

The effect of the yield number on the flowfield structure is demonstrated in Fig. 3, where the streamlines are shown for three different yield numbers. In general the flowfield in the current geometry consists of three distinct flow domains. The first is that appearing close to the inlet section, where the effect of the contraction plane is weak or non-existent, and thus fully developed conditions prevail, as indicated by the parallel to the wall streamlines. The second is the domain where the

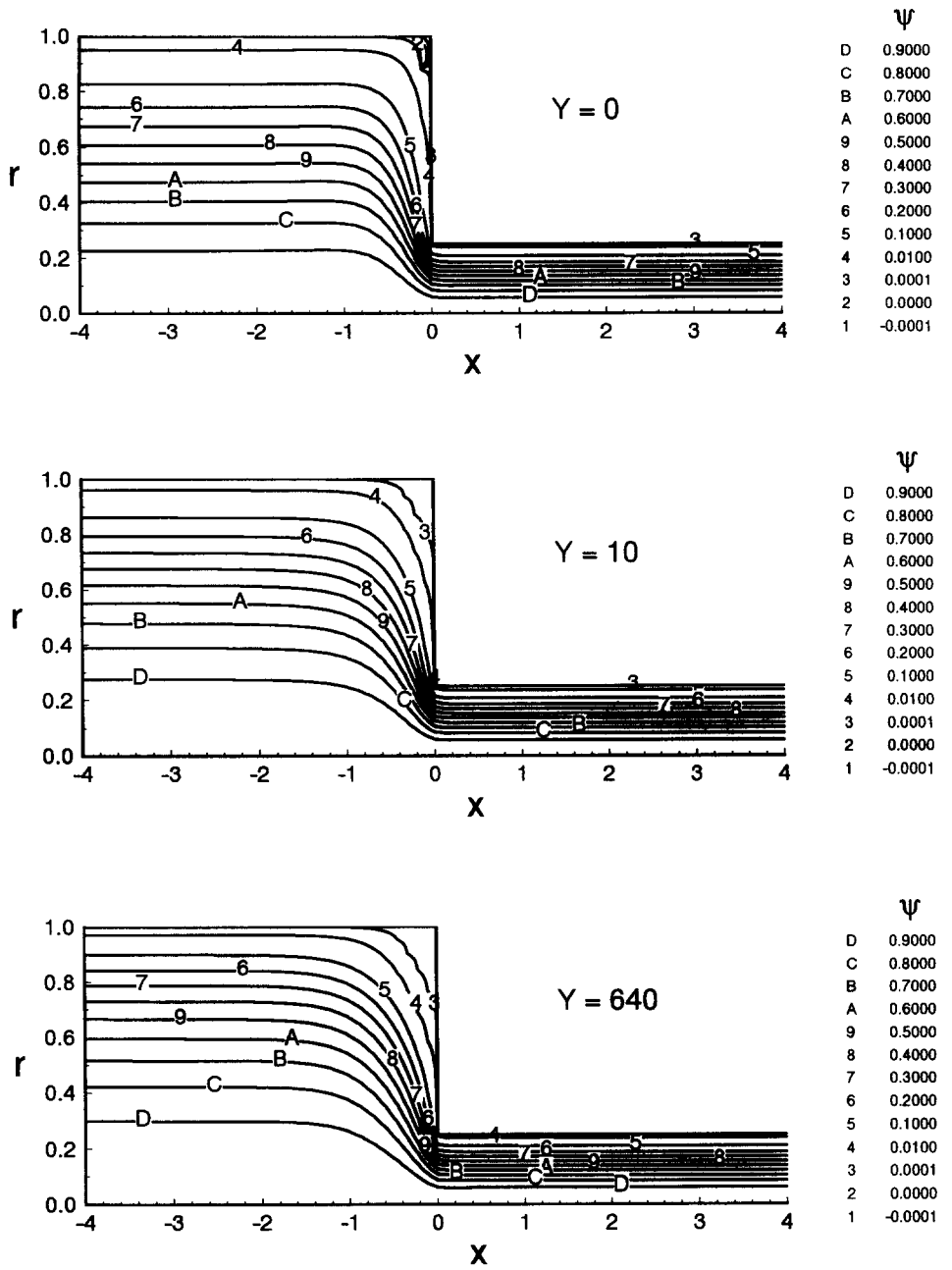

Fig. 3. Flow field streamlines for $Y = 0$, 10 and 640.

effect of the contraction plane is dominant, i.e. the corner and the vicinity of the inlet to the smaller pipe. This domain is characterized by the displacement of the streamlines towards the centerline as the contraction plane is approached. In the Newtonian case, as seen in Fig. 3(a), a separated flow region forms. The detachment length is approximately 1/3 the large pipe radius upstream of the contraction plane. This is consistent with what has been reported earlier (see Boger [3] and Kim-E *et al.* [4]). In the vicinity of the centerline the flow accelerates rapidly as the throat is approached. As the smaller diameter pipe element is entered, the flow rapidly evolves to the corresponding fully developed flow conditions, i.e. the third flow domain. The corresponding streamlines in the case of the flow of a viscoplastic fluid at $Y = 10$ is shown in Fig. 3(b). Again, similar features are observed except that no separation is observed close to the 90° corner where, in this case, the flow comes practically to a dead stop. As the yield number increases from zero to low values, the extent of this secondary flow region rapidly decreases. Numerical experimentation shows that it ceases to exist at a yield number of about one. Increasing the yield number results in the growth of this semi-stagnant zone. However, as the yield number is further increased to a value of $Y = 640$ [see Fig.

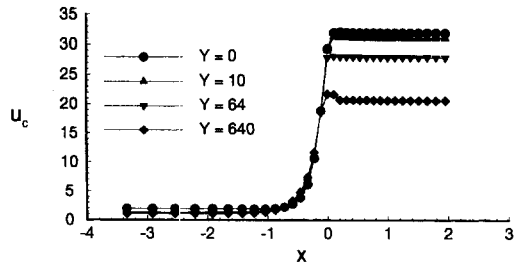

Fig. 4. Effect of yield number on the evolution of the centerline velocity.

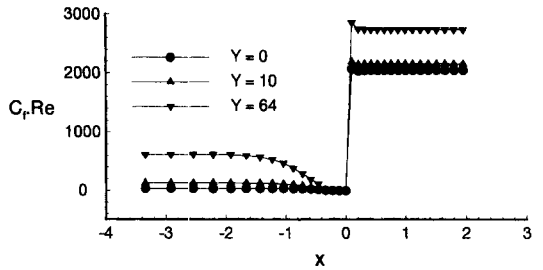

Fig. 5. Effect of yield number on the friction coefficient distribution.

3(c)], the growth of the semi-stagnant region does not increase appreciably. Numerical experimentation shows that the length of this domain reaches an asymptotic value of 1.0 R_w as $Y \to \infty$.

In the case of Newtonian fluids it has been established that the evolution of the streamwise component of the velocity along the centerline in the immediate vicinity of the plane of contraction is for all practical purposes independent of the Reynolds number for $Re \leqslant 1$ and independent of the contraction ratio for $\beta \geqslant 4$ and low Re. Kim-E *et al.* [4] showed that this evolution is also independent of the power law index in the case of non-Newtonian shear thinning fluids. The present study establishes a similar fact for the case of Bingham fluids where the effect of the yield number is minimal resulting in indistinguishable curves as can been seen in Fig. 4. Upstream of this region, the centerline velocity depends on the yield number since the fully developed profiles at the inlet differ with Y. The centerline velocity evolution is also different downstream where the fully developed values also vary with Y. Notice that in this region the differences are more pronounced than upstream. This is due to the fact that the differences of the profiles upstream are not significant given that for $Y > 10$, the profiles are fairly insensitive to yield number variations. However, downstream of the contraction the bulk velocity is 16 times of that upstream and the effective yield number is 1/64 of the value upstream (which are used here as the reference). As a result the effective yield numbers are lower in the smaller pipe and thus, the substantial variations depicted in this figure.

Figure 5 shows the axial variation of the friction coefficient, C_f, with Y. As shown, increasing yield numbers result in increasing friction coefficients both upstream and downstream of the contraction plane. This trend is expected due to the thinning of the shearing layer close to the wall with the yield number. Again, this thinning effect is less pronounced in the downstream portion of the confining geometry due to the strong shearing influence of the smaller radius wall which tends to suppress the yield stress related behavior. Close to the contraction plane the effect of the very low rates of deformation zone is characterized by the sudden drop in the value of C_f. The influence of the contraction section is felt further upstream of the contraction plane for fluids with higher yield numbers, as evidenced in the earlier drop of the C_f values from the fully developed ones at the inlet. This is attributed to the higher effective viscosities associated with higher yield numbers. It should be noticed again that the friction coefficient evolution in the immediate vicinity of the contraction plane is independent of the yield number.

A significant portion of the hydrodynamic characteristics of the flowfields in sudden circular contractions could be easily revealed by studying the evolution of the profiles of the streamwise component of the velocity. As seen in Fig. 6(a), in the case of a Newtonian fluid, the profile initially flattens out due to the deceleration of the flow along the centerline caused by a positive pressure gradient upstream of the contraction. Then, very close to the contraction plane, the velocity is negative near the wall and rapidly increasing in value along the centerline up to the plane of the throat. At the throat, the profile is not flat given the very rapid propagation of the wall influence towards the centerline for creeping flows. After that it evolves with the velocities close to the wall decreasing and the ones close to the centerline increasing to their asymptotic values. The effect of the existence of a yield stress is evident both in the upstream and downstream portions of the geometry, as can be seen in Fig. 6(b). Upstream, the *core-flow* region dissipates as the throat is approached due to severe flow acceleration. As mentioned earlier there are no regions of negative velocities (due to the disappearance of the corner vortices). Downstream of the contraction, the velocity profile evolves towards its fully developed shape faster close to the wall than close to the centerline. This is consistent with the earlier observations of Vradis *et al.* [14]. As the flow develops a new *core-flow* region appears, the size of which increases with increasing yield numbers. Notice that the velocity profiles in the developing flow region downstream of the throat are not very sensitive to the yield number since, as explained earlier, the characteristics of the flow field in this area are Newtonian-like given the very high rates of deformation. This last fact also explains the overshoots in the centerline velocity evolution right downstream of the contraction plane. Given the Newtonian-like behavior of the flow, the velocity profile at the entrance of the smaller pipe is independent of the yield number. For a Newtonian fluid this profile will

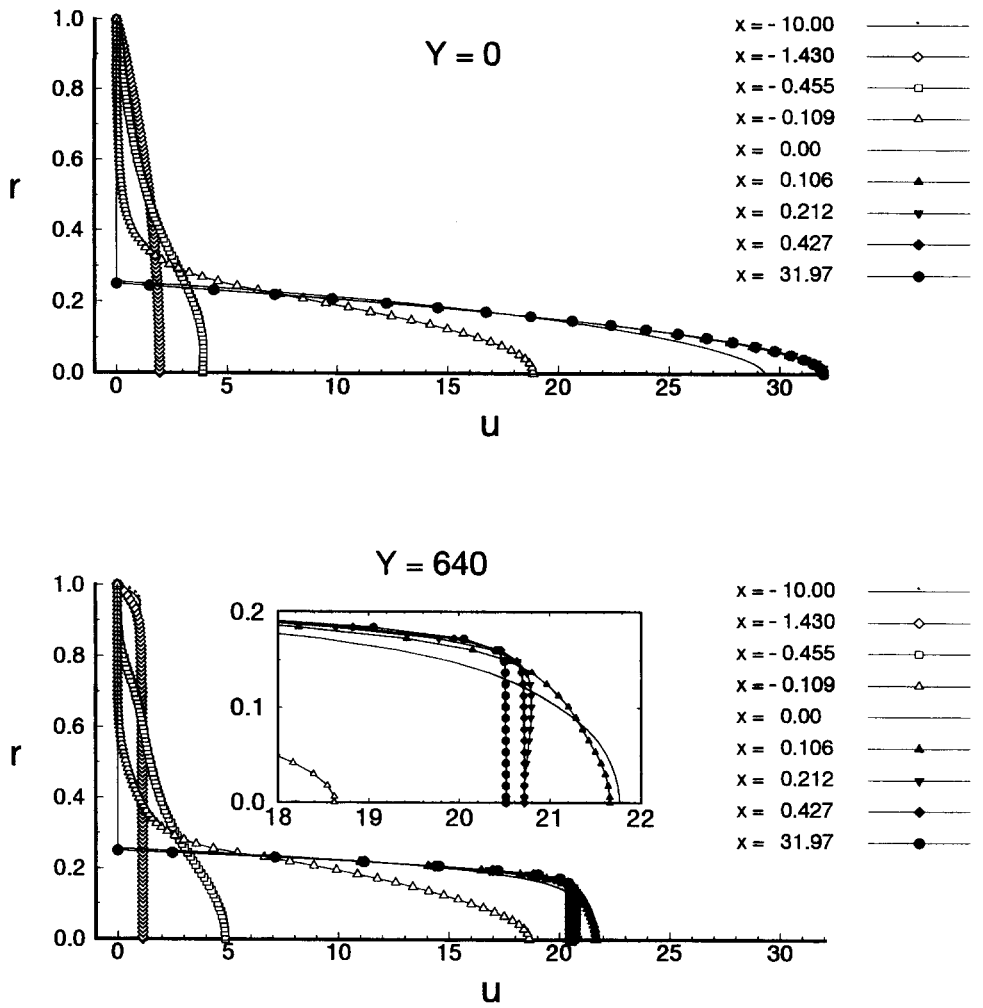

Fig. 6. Effect of yield number on the development of the profiles of the axial component of the velocity.

eventually evolve to the parabolic distribution of the Poiseuille flow in which the centerline velocity is twice the bulk one. However, for Bingham fluids the fully developed centerline velocity value is decreasing with the yield number. Thus, as the yield number increases the centerline velocity experiences an increasingly higher drop from that at the entrance to the small pipe as fully developed conditions are approached.

The wall temperature is maintained constant and equal to the temperature of the incoming fluid. Under these conditions, the only phenomenon resulting in the appearance of temperature gradients is the heat generated due to viscous dissipation. It is, therefore, imperative to study the distribution of the viscous dissipation term in the energy equation throughout the flowfield, since it is this term that derives the heat transfer phenomena studied here. In the case of a Newtonian fluid (see Fig. 7(a), $Y = 0$) and close to the inlet, there is a monotonic increase in the value of the dissipation term Φ from the centerline, where it attains very low values due to relatively low rates of deformation, to the wall, where it attains a maximum value due to the high rates of deformation near the wall. As the contraction plane is approached and near the wall close to the corner there exists a recirculating flow region characterized by low rates of deformation and consequently low values of the dissipation function. However, in the vicinity of the entry to the small diameter pipe the flow acceleration results in very high rates of deformation and consequently in very high values of Φ. As the smaller pipe is entered, the hydrodynamic field develops rapidly resulting in a distribution of Φ similar to that at the inlet of the larger pipe with overall values, however, much higher due to the increase shear which results from the increase in bulk velocity. In the case of a Bingham fluid and for $Y = 64$ [see Fig. 7(b)], the existence of a core-flow (i.e. undeforming) region upstream results in a corresponding zone of very low (for an ideal Bingham plastic, zero) values of the dissipation function. In the region where velocity gradients are sustained, the shear is higher than that in the case of a Newtonian fluid and as a result the transition zone in the radial direction from very low values to the maximum value

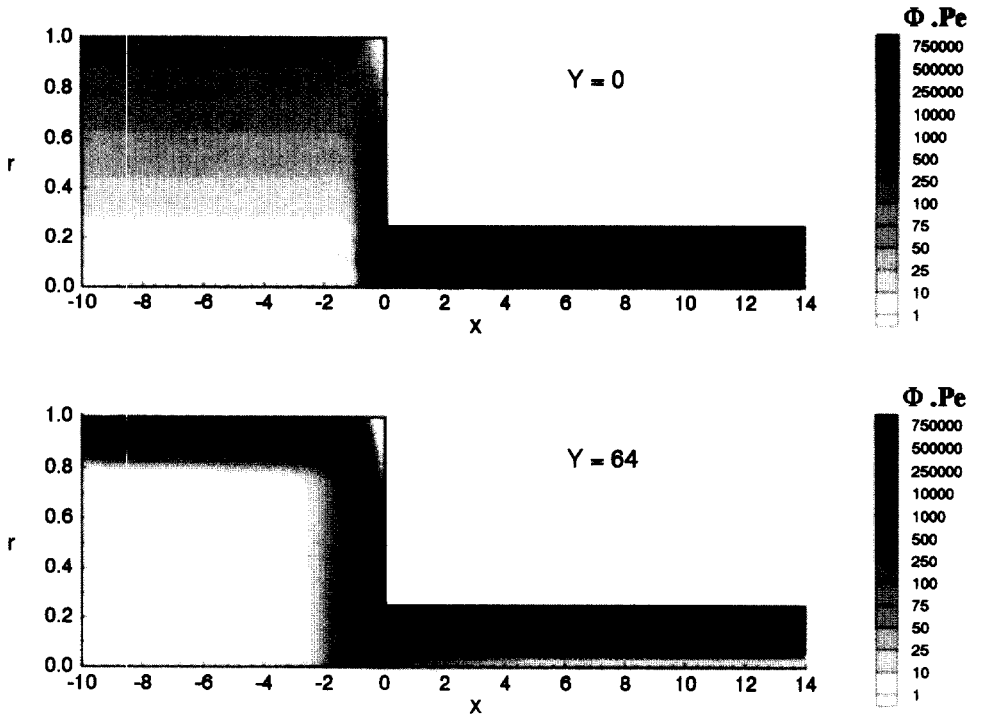

Fig. 7. Effect of yield number, Y, on contours of the viscous dissipation term.

at the wall takes place in a much narrower zone. At the corner, the existence of the near stagnant zone results in a corresponding zone of low values of Φ. Near the inlet to the small pipe the flow, as explained earlier, is Newtonian-like, thus resulting in nearly identical Φ distributions. In the small pipe, the distribution of Φ is similar to that in the entry of the upstream pipe given the appearance of a core-flow region along the axis which results in a corresponding zone of practically zero rates of viscous dissipation. Close to the wall high values of Φ are experienced again due to the high shear rates.

With this information available, it is now much easier to understand the temperature and Nusselt number distributions. The evolution of the temperature profile due to viscous heating is both qualitatively and quantitatively described in Fig. 8 for varying yield and Peclet numbers. In the case of a Newtonian fluid the relatively low levels of shear result in a very small increase in temperature upstream of the contraction plane and close to the inlet, as seen in Figs. 8(a) and (b). The heat generated due to the viscous dissipation is either convected away at the wall or conducted into the interior of the flow domain toward the centerline. As expected the temperature rise away from the wall is higher in the case of the low Peclet number [Fig. 8(a), $Pe = 1$] since the increased effects of convective cooling in the case of $Pe = 100$ [Fig. 8(b)] tend to decrease the temperature levels. In the immediate vicinity of the contraction plane and close to the inlet of the smaller pipe the very high values of the viscous dissipation function result in substantial increases in temperature. Again, the temperatures are high in the case of the low Peclet number since the heat transfer to the walls is dominated by conduction rather than convection. It is important to notice here the very high temperature gradients along the contraction wall. In the smaller pipe, the higher amounts of heat dissipated result in a further increase in temperature, which within a certain distance from the throat reaches a fully developed distribution. This distance increases with the Peclet number as is already well established. For a Bingham fluid with $Y = 10$, the higher values of the viscous dissipation function result in temperature increases close to the inlet greater than those in the case of the Newtonian fluid, as can be seen in Figs. 8(c) and (d). The effect of the Peclet number is similar to that in the Newtonian case. Close to the contraction plane the flow is Newtonian like and as a result so is the temperature distribution. The same is true in this case for the flow in the smaller diameter pipe, as explained earlier. A further increase in the value of the yield number to $Y = 640$ results in further increases of the temperature upstream of the contraction and smaller thermal entrance lengths in the smaller pipe [see Figs. 8(e) and (f)], as has been already established by Vradis *et al.* [14] [notice that the contour colors of Figs. 8(e) and (f) are different than those in Figs. 8(a)–(d)].

Very informative is the bulk temperature distribution in the flow as depicted in Fig. 9(a) and (b) for two Peclet numbers. The entrance effects at the inlet result in the rapid increase of the bulk temperature, followed by a region of constant values due to the development of the flow. As the contraction is approached the temperature rises rapidly again. In the

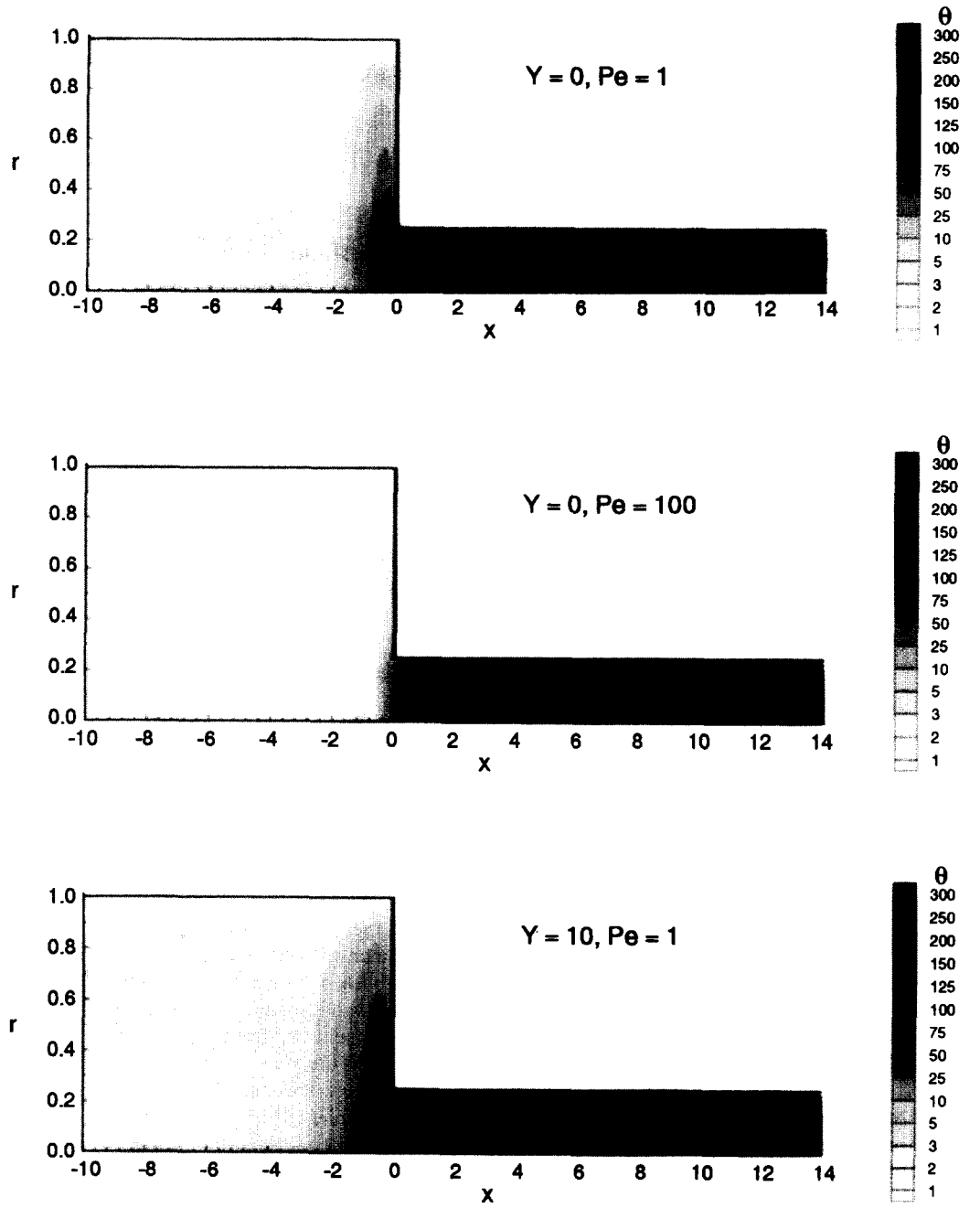

Fig. 8. Effect of yield and Peclet, Y and Pe, numbers on the temperature contours.

case of a low Peclet number, it reaches a maximum value at the throat, while in the case of the higher Peclet number it continues to rise as the fluid enters the smaller pipe due to the higher rates of cooling along the contraction plane in this case. Due to the phenomena involved, which were explained earlier, this bulk temperature rise increases with the yield number.

Finally, Figs. 10(a) and (b) show the Nusselt number distribution along the wall for two different values of the Peclet number of $Pe = 1$ and 100. As expected, a peak value appears at the inlet section (very rapid thermal field development) followed by a domain of more or less constant Nusselt numbers due to the developed hydrodynamic and thermal fields region in the middle portion of the large (upstream) pipe. As the contraction wall is approached, its influence results in an initially gradual and then rapid reduction in the Nusselt number, occurring at $x = -3$ for Newtonian fluids and increasing with yield number for Bingham plastics up to $x = -5$ for $Y = 640$ in the case of $Pe = 1$. At $Pe = 100$, however, this influence starts at $x = -1$ for a Newtonian fluid and increases up to $x = -3$ for $Y = 640$. At the corner the Nusselt num-

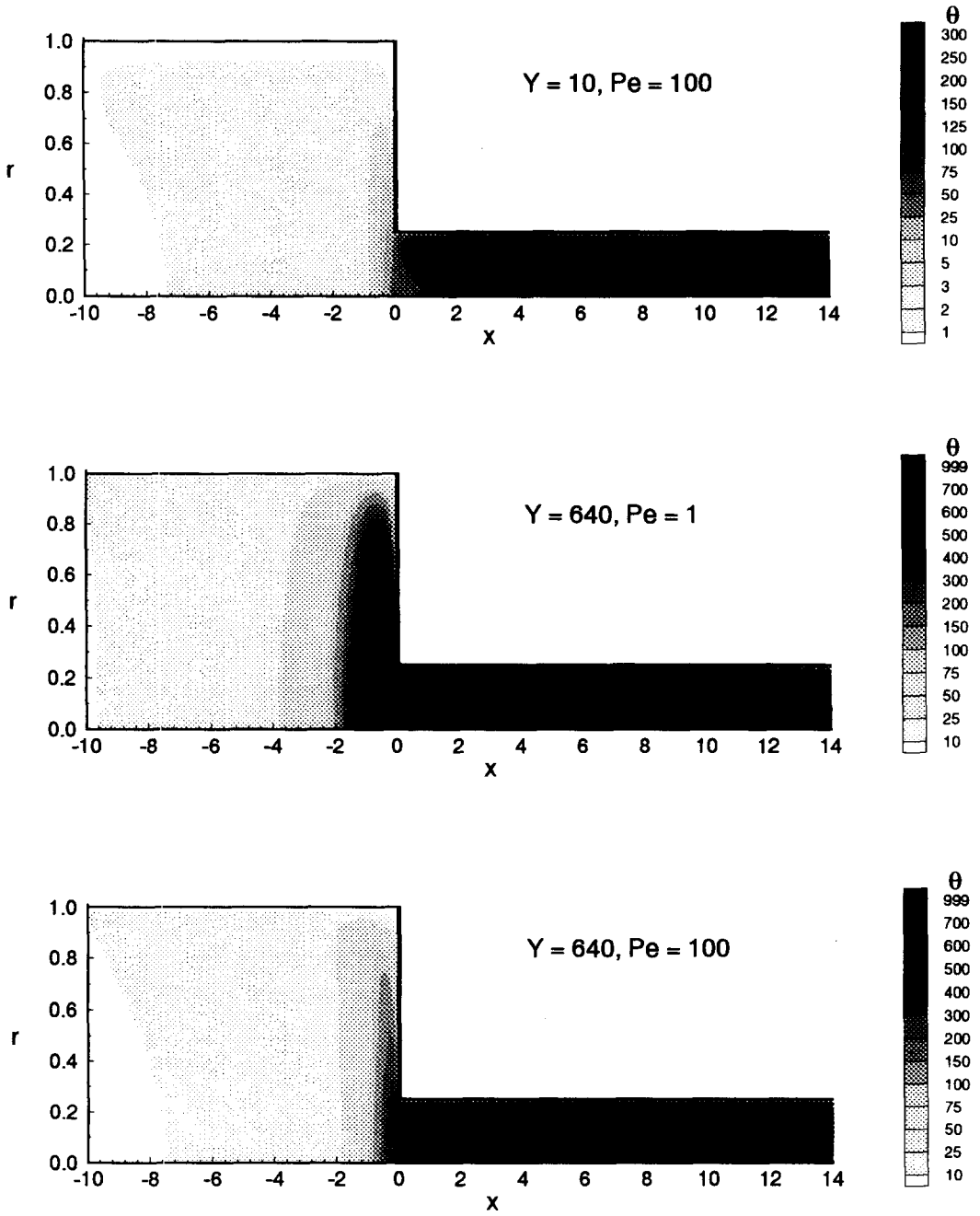

Fig. 8.—*Continued.*

ber reaches a value of zero. As the smaller pipe is entered a local maximum of the Nusselt number is observed in all cases due to the entrance effects. This value increases with the Peclet number as anticipated based on the work of Vradis *et al.* [14]. Again, the Newtonian like nature of the flow near the contraction leads to a collapse of all the curves for different yield numbers into one in the immediate vicinity of the contraction plane. Thus, the heat transfer characteristics near the corner depend on the Peclet number only, and are independent of the yield number. Far away from the contraction plane, both upstream and downstream, the Nusselt number increases with the yield number for all Peclet numbers. This is consistent, once more, with the observations of Vradis *et al.* [14] and is explained by the increase in the rates of heat removal associated with higher velocity gradients, at higher yield numbers, in the region close to the wall. The variation of the Nusselt number with the yield number in the fully developed flow regime and for high yield numbers can be expressed in a power law form, the exponent being equal to 1/2, i.e. $Nu \sim Y^{1/2}$. It should be noted that the same behavior has been established for the Sherwood number variation with

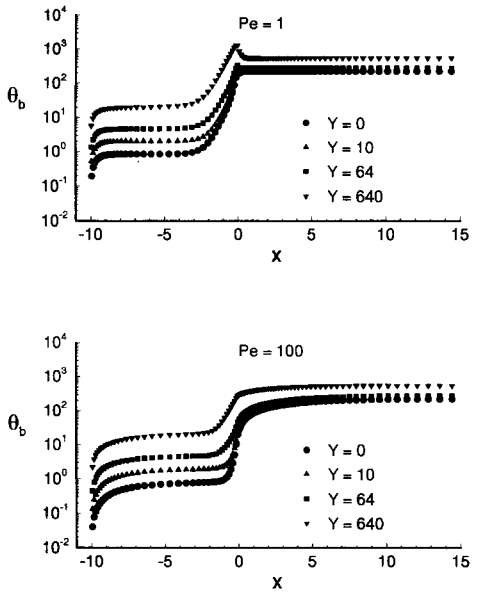

Fig. 9. Effect of yield and Peclet numbers on the bulk temperature distribution.

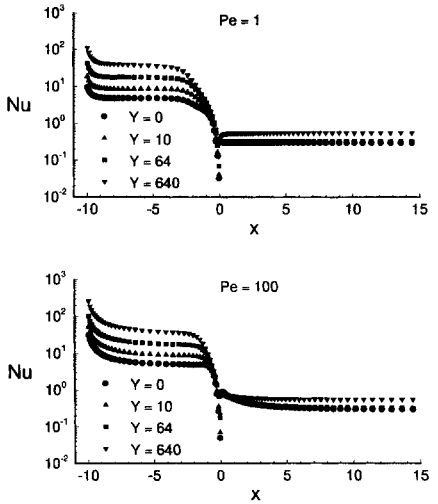

Fig. 10. Effect of yield and Peclet numbers on the Nusselt number distribution.

the yield number in the case of the flow of a sphere in a Bingham fluid (see Beris *et al.* [26]), the power exponent attaining the value of 1/6.

CONCLUSIONS

The non-isothermal creeping flow of a viscoplastic Bingham fluid through an axisymmetric sudden contraction has been analyzed using a finite-differences based numerical technique. The contraction ratio was fixed at four while a wide range of yield numbers and Peclet numbers were studied. The generated thermal field is entirely due to viscous heating. The results establish the disappearance of the corner vortex at very low yield numbers and the independence of the flow characteristics from the yield number in the immediate vicinity of the contraction plane, where the flow is practically Newtonian-like. It is also shown that the characteristics of the thermal field are sensitive to the yield and Peclet numbers. Viscous heating is significant in the immediate vicinity of the contraction, with its significance diminishing with increasing Peclet number.

Acknowledgements—The support of the Exxon Educational Foundation for this project is hereby acknowledged.

REFERENCES

1. J. P. Burke and N. S. Berman, ASME Publication, No. 69-WA/FE13 (1969).
2. A. V. Ramamurthy and J. C. H. McAdam, *J. Rheology* **24,** 167–188 (1980).
3. D. V. Boger, Viscoelastic flows through contractions, *Ann. Rev. Fluid Mech.* **19,** 157–182 (1987).
4. M. E. Kim-E, R. A. Brown and R. C. Armstrong, The roles of inertia and shear-thinning in flow of an inelastic liquid through an axisymmetric sudden contraction, *J. Non-Newtonian Fluid Mech.* **13,** 341–363 (1983).
5. S. A. White, A. D. Gostis and D.G. Baird, Review of the entry flow problem: experimental and numerical, *J. Non-Newtonian Fluid Mech.* **24,** 121–160 (1987).
6. R. B. Bird and G. C. Dai, The rheology and flow of viscoplastic materials, *Rev. Chem. Engng* **1**(1), 1–70 (1983).
7. J. T. Park, R. J. Mannheimer, T. A. Grimley and T. B. Morrow, Pipe flow measurements of a transparent non-Newtonian slurry, *J. Fluids Engng* **11,** 331–336 (1989).
8. D. J. Wildman, J. M. Ekmann, J. R. Kadambi and R. C. Chen, Study of the flow properties of slurries using the refractive index matching techniques and LDV, *Powder Technol.* **73,** 211–218 (1992).
9. G. C. Vradis and M. V. Otugen, The flow of Bingham plastics over a sudden expansion in a pipe. In *Recent Advances in Non-Newtonian Flows*, ASME AMD-Vol. 153/PED-Vol. 141, pp. 129–136 (1992).
10. P. S. Scott and F. Mirza, Finite-element simulation of laminar viscoplastic flows with regions of recirculation, *J. Rheology* **32**(4), 387–400 (1988).
11. S. S. Abdali and E. Mitsoulis, Entry and exit flows of Bingham fluids, *J. Rheology* **36**(2), 389–407 (1992).
12. T. C. Papanastasiou, Flow of materials with yield, *J. Rheology* **31**(5), 385–404 (1987).
13. A. B. Samant and W. J. Marner, Heat transfer to a Bingham plastic in the entrance region of a circular tube, *Nucl. Sci. Engng* **43,** 241–246 (1971).
14. G. C. Vradis, J. Dougher and S. Kumar, Entrance pipe flow and heat transfer for a Bingham plastic, *Int. J. Heat Mass Transfer* **36**(3), 543–552 (1993).
15. P. Payvar, Asymptotic Nusselt numbers for dissipative non-Newtonian flow through ducts, *Appl. Sci. Res.* **27,** 297–306 (1973).
16. E. H. Wissler and R. S. Schechter, The Graetz–Nusselt problem (with extension) for a Bingham plastic, *Chem. Engng Prog. Symp. Ser.* 29 **55,** 203–208 (1959).
17. G. Forrest and W. L. Wilkinson, Laminar heat transfer to temperature-dependent Bingham fluids in tubes, *Int. J. Heat Mass Transfer* **16,** 2377–2391 (1973).
18. P. R. Johnston, Axial conduction and the Graetz problem for a Bingham plastic in laminar tube flow, *Int. J. Heat Mass Transfer* **34**(4/5), 1209–1217 (1991).
19. V. D. Murty, Nonisothermal flows of Bingham plastics, ASME HTD-Vol. 79, pp. 33–38 (1987).
20. E. Mitsoulis, S. S. Abdali and N. C. Markatos, Flow simulation of Herschel–Bulkley fluids through extrusion dies, *Can. J. Chem. Engng* **71,** 147–160 (1993).

21. R. B. Bird, W. E. Stewart and E. N. Lightfoot, *Transport Phenomena*, pp. 101–104. Wiley, New York (1960).
22. G. C. Vradis and L. Van Nostrand, Laminar coupled flow downstream of an axisymmetric sudden expansion, *J. Thermophys. Heat Transfer* **6**(2), 288–295 (1992).
23. E. J. O'Donovan and R. I. Tanner, Numerical study of the Bingham squeeze film problem, *J. Non-Newtonian Fluid Mech.* **14**, 75–83 (1984).
24. G. G. Lipscomb and M. M. Denn, Flow of Bingham fluids in complex geometries, *J. Non-Newtonian Fluid Mech.* **14**, 337–346 (1984).
25. C. R. Beverly and R. I. Tanner, Numerical analysis of three-dimensional Bingham plastic flow, *J. Non-Newtonian Fluid Mech.* **42**, 85–115 (1992).
26. A. N. Beris, J. A. Tsamopoulos, R. C. Armstrong and R. A. Brown, Creeping motion of a sphere through a Bingham plastic, *J. Fluid Mech.* **158**, 219–244 (1985).